Check for updates

Local Sphingosine Kinase 1 Activity Improves Islet Transplantation

Darling Rojas-Canales,[1,2] Daniella Penko,[1,2] Kay K. Myo Min,[3] Kate A. Parham,[3] Heshan Peiris,[4,5] Rainer V. Haberberger,[6] Stuart M. Pitson,[3] Chris Drogemuller,[1,2] Damien J. Keating,[4,5,7] Shane T. Grey,[8] Patrick T. Coates,[1,2] Claudine S. Bonder,[1,3] and Claire F. Jessup[1,5,6]

Diabetes 2017;66:1301–1311 | DOI: 10.2337/db16-0837

Pancreatic islet transplantation is a promising clinical treatment for type 1 diabetes, but success is limited by extensive β-cell death in the immediate posttransplant period and impaired islet function in the longer term. Following transplantation, appropriate vascular remodeling is crucial to ensure the survival and function of engrafted islets. The sphingosine kinase (SK) pathway is an important regulator of vascular beds, but its role in the survival and function of transplanted islets is unknown. We observed that donor islets from mice deficient in SK1 (*Sphk1* knockout) contain a reduced number of resident intraislet vascular endothelial cells. Furthermore, we demonstrate that the main product of SK1, sphingosine-1-phosphate, controls the migration of intraislet endothelial cells in vitro. We reveal in vivo that *Sphk1* knockout islets have an impaired ability to cure diabetes compared with wild-type controls. Thus, SK1-deficient islets not only contain fewer resident vascular cells that participate in revascularization, but likely also a reduced ability to recruit new vessels into the transplanted islet. Together, our data suggest that SK1 is important for islet revascularization following transplantation and represents a novel clinical target for improving transplant outcomes.

Islet transplantation is a potential curative therapy for type 1 diabetes (1); however, its success is limited by the significant loss of β-cell mass and function posttransplantation (2,3). Removal of islets from their rich and specialized blood supply immediately triggers cellular changes, inducing a relative hypoxia in β-cells and an altered phenotype of other islet cells including immune cells and endothelial cells (ECs) (4,5). Furthermore, additional factors that are detrimental to islet graft survival and function include poor revascularization, cytokine-induced apoptosis, immediate blood-mediated inflammatory response, and reoccurrence of autoimmune responses (3). Therefore, there is a need to identify key drug targets to improve the function and survival of islets posttransplantation.

In the native pancreas, intraislet vascular ECs are critical for islet function: not only do they provide a conduit for blood delivery, but also their intimate association with β-cells provides direct regulatory and supportive factors (6,7). Despite accounting for only 1 to 2% of pancreatic mass, islets receive 10% of the overall pancreatic blood flow (8). Posttransplantation, islet revascularization typically takes up to a month to develop, and the resultant vasculature is often aberrant compared with native islets in the pancreas (9). We have previously shown that intraislet vascular ECs are rapidly lost from donor islets and that cotransplantation of vascular progenitor cells can improve transplant success in a marginal model (10). In addition, resident donor intraislet ECs persist in the functional vasculature of transplanted islets (11,12), suggesting that pathways controlling vascular cell fate are likely to be important following islet transplantation.

[1]Discipline of Medicine, The University of Adelaide, Adelaide, Australia
[2]Central Northern Adelaide Renal and Transplantation Services, Royal Adelaide Hospital, Adelaide, Australia
[3]Centre for Cancer Biology, University of South Australia and SA Pathology, Adelaide, Australia
[4]Department of Human Physiology, Flinders University, Bedford Park, Australia
[5]Centre for Neuroscience, Flinders University, Bedford Park, Australia
[6]Department of Anatomy & Histology, Flinders University, Bedford Park, Australia
[7]South Australian Health and Medical Research Institute, Adelaide, Australia
[8]Garvan Medical Institute, Darlinghurst, Australia

Corresponding authors: Claudine S. Bonder, claudine.bonder@unisa.edu.au, and Claire F. Jessup, claire.jessup@flinders.edu.au.

Received 9 July 2016 and accepted 2 February 2017.

© 2017 by the American Diabetes Association. Readers may use this article as long as the work is properly cited, the use is educational and not for profit, and the work is not altered. More information is available at http://www.diabetesjournals.org/content/license.

The ubiquitous sphingosine kinase (SK) pathway plays a complex role in the regulation of many vascular beds throughout the body. The SKs are highly conserved lipid kinases in the sphingolipid pathway that catalyze the phosphorylation of sphingosine to form sphingosine-1-phosphate (S1P) (13). Two SK isoforms have been identified, cloned, and characterized (SK1 and SK2). They differ in subcellular localization patterns and distribution in adult tissue and have both overlapping and distinct biological functions (13). Mice lacking either SK gene (*Sphk1* or *Sphk2*) are viable, fertile, and phenotypically normal (14,15), but deletion of both genes causes embryonic lethality because of severe defects in angiogenesis and neurogenesis (15). Increasing evidence suggests that maintaining S1P homeostasis is important for preventing unwanted immune responses (16,17) and to retain appropriate vascular barrier integrity (18). Although the basal level of intracellular S1P is generally low, biological stimuli (e.g., tumor necrosis factor-α) can increase its production via transient activation of SK1 through its phosphorylation by extracellular signal–regulated kinases 1 and 2 (19). Extracellular S1P binds to a family of G-protein–coupled receptors (S1P receptors 1–5) that induce downstream signaling, such as phosphatidylinositol 3 kinase/Akt and extracellular signal–regulated kinases 1 and 2 (20), and receptors S1P receptors 1–3 are expressed on ECs (21,22).

There is increasing evidence that the SK/S1P axis plays an important role in type 1 diabetes and islet cell function, with the sphingolipid rheostat implicated in the balance between cell proliferation and apoptosis (23). However, its importance for islet transplantation is unknown. The SK pathway may affect islet transplantation directly by affecting β-cell function or modulating β-cell survival or, more indirectly, by controlling islet revascularization. This study examines the specific role that SK1 plays in islet function and engraftment posttransplantation.

RESEARCH DESIGN AND METHODS

Islet Isolation

All experimental procedures were approved by the Animal Ethics Committee of the University of Adelaide and conform to the Australian Code of Practice for the Care and Use of Animals for Scientific Purpose. Pancreatic islets were isolated from 7–16-week-old male C57B6 mice (University of Adelaide Laboratory Animal Services, South Australia, Australia) or from *Sphk1* knockout (KO) (14) or wild-type (WT) mice on a C57Bl6 background exactly as we have described (10).

Flow Cytometry

Handpicked islets were dissociated with Accutase (400–600 units/mL; Sigma-Aldrich) in a 37°C water bath for 5 min as previously described (10). Dispersed islets were resuspended in 100 μL (PBS with 0.1% FCS) and incubated with mouse Fc block (BD Pharmingen) for 10 min at 4°C. Anti–CD31-PE (clone MEC13.3; BD Biosciences) was added and incubated for 30 min at 4°C. Rat IgG2a-PE (BD Biosciences) was used as an isotype control. FACSCanto II (BD Biosciences) was used to collect data, and samples were then analyzed on FCS Express v.3 software (De Novo Software, Los Angeles, CA).

Quantitative Real-time PCR

Islets were cultured (0, 6, 24, and 48 h) at 37°C, 5% CO_2. Samples were washed with PBS and resuspended in RNA lysis buffer, and RNA was extracted (RNA Mini Kit; Qiagen). Samples were reverse-transcribed into cDNA using the iScript Reverse Transcription Supermix for quantitative real-time PCR (Bio-Rad). Predesigned TaqMan primers used to detect cDNA transcribed from *Sphk1*, *Vegfa*, and *kdr* (vascular endothelial growth factor [VEGF] receptor 2) mRNA (Applied Biosystems). Primer mix (0.5 μL of 20×) was add to 5 μL of 2× Universal Master Mix (Applied Biosystems) and mixed with 5–10 ng cDNA (10 μL final reaction volume). PCR cycling conditions were: initial hold for 10 min at 95°C (polymerase activation), 42 cycles at 95°C for 15 s (denature), and 60°C for 60 s (annealing/extending). PCR was carried out using a Rotorgene system (Qiagen). Gene expression was normalized to β_2-*microglobulin* or *Gapdh* expression (24,25).

Real-time Cell Analysis Migration Assay and Cell Viability

Cell migration experiments were performed using 16-well plates (CIM-Plate16; ACEA Biosciences, Inc.). Each well consists of a modified Boyden chamber containing a microporous membrane (8-μm pores). Microelectrodes attached to the underside of the membrane allow impedance-based detection of migrated cells via the xCELLigence Real-Time Cell Analysis (RTCA) DP Instrument (ACEA Biosciences, Inc.). Prior to each experiment, MS1 cells, pancreatic islet ECs transformed by infection with a temperature-sensitive SV40 large T antigen (tsA-58–3; American Type Culture Collection, Manassas, VA) (26), were grown overnight in low serum (1% FCS), washed, and resuspended in serum-free DMEM with or without S1P receptor inhibitor (VPC23019 10 μmol/L; Avanti Polar Lipids, Alabaster, AL) for 30 min at room temperature (RT). Serum-free DMEM was added to the upper (160 μL/well) and lower (30 μL/well) wells, and the plate was locked into the RTCA DP Instrument at 37°C and 5% CO_2 for 60 min to obtain equilibrium and an initial background measurement. MS1 cells (3×10^4/well) were added to the upper wells in 100 μL serum-free DMEM and allowed to settle at RT for 30 min prior to the initiation of the programmed signal detection schedule. Lower wells containing serum-free DMEM were used to control for background cell migration. Lower wells with DMEM containing VEGF-A (25 ng/mL) or FCS (20%) were used as positive controls for each experiment. S1P (1 μmol/L in methanol [diluted 1:1,000 in serum-free media]) or vehicle (diluted methanol; 0.1% [volume for volume]) was added as 160 μL to the lower (empty) well of appropriate samples. Impedance data were recorded every 5 min for 12 h and then every 15 min for 24 h with RTCA software supplied. Cell index

measurements for each well were normalized to the initial readings following cell addition and settling. Cell migration rates were calculated by fitting a linear regression model (Prism; GraphPad Software) to the raw data over the first 6 h and comparing slope values. Total cell migration was estimated by calculating the area under the curve (AUC) values (Prism; GraphPad Software) of normalized data over 12 h.

Cell viability was determined via Annexin V/7-aminoactinomycin D (7-AAD) staining and flow cytometric analysis. MS1 cells were incubated for 12 h with the vehicle control, S1P (1 μmol/L), or the S1P antagonist VPC23019 (10 μmol/L) at 37°C and 5% CO_2. Cells were then labeled with an antibody to Annexin V (1:5 in 1× binding buffer; BD Biosciences) for 15 min at RT prior to incubation with 7-AAD (1:20 in 1× binding buffer; BD Biosciences). Cells were washed, resuspended in 1× binding buffer, and analyzed on the Accuri flow analyzer (BD Biosciences). Data were further analyzed using FCS Express 4 Flow Cytometry: Research Edition (De Novo Software).

Intraperitoneal Glucose Tolerance Test

Mice were fasted (4 h) and given 2 mg/kg glucose by intraperitoneal injection. Tail vein blood samples were taken prior to injection and at 15, 30, 60, and 120 min postinjection. Blood glucose level (BGL) was determined with a glucometer (Optium; Abbott Diabetes Care, Victoria, Australia).

Glucose Stimulation Insulin Secretion Assay

Islets were handpicked into basal Krebs buffer (3 mmol/L glucose) at 37°C. Groups of 10 islets were transferred into fresh basal Krebs buffer (3 mmol/L glucose) at 37°C for 1 h, and supernatant was collected. Islets were resuspended in 20 mmol/L glucose Krebs buffer (high) at 37°C for 10 min (first phase); supernatant was collected, and islets were resuspended in fresh Krebs buffer (20 mmol/L glucose) at 37°C for 1 h (second phase). Following recovery (1 h), islets were incubated with high-potassium Krebs buffer (70 mmol/L) at 37°C for 30 min, and supernatant was collected. Supernatants were analyzed for insulin using the Ultra-Sensitive Mouse Insulin ELISA Kit (low-range assay; Crystal Chem Inc., Downers Grove, IL).

Islet Transplantation Under the Kidney Capsule

C57B6 mice (8–12 weeks old) were rendered diabetic by intraperitoneal injection of 200 mg/kg streptozotocin in citrate buffer. BGLs were monitored daily, and diabetes was confirmed by two consecutive blood glucose readings >16.6 mmol/L. Diabetic mice were transplanted on day 5 after the readings (provided that the BGLs were >16.6 mmol) with a minimal mass (200 islets) of cultured islets under the kidney capsule. BGLs were monitored daily (A.M.) posttransplant. Cure of diabetes was defined as the first day of two consecutive nonfasted blood glucose readings of <11.1 mmol/L with no subsequent sustained reversion to hyperglycemia.

Histological Examination of Islet Number and Size

Pancreata of 16-week-old mice were collected and fixed (10% buffered formalin). The tissue was bisected transversely and the tail portion processed for routine paraffin wax embedding and histological sectioning (Flinders Microscopy Suite, Flinders University, Bedford Park, South Australia). Sections (8 μm) were cut in the transverse plane from the center of the tail portion. Four sections per pancreata (spaced throughout the specimen) were processed for insulin staining and examined at the fluorescence microscope (AX70; Olympus). Hematoxylin and eosin were used to confirm equivalent pancreata sampling location between specimens. Images were merged using ImageJ software (National Institutes of Health) and the composite image automatically processed using an in-house macro program to count the number of labeled islets and calculate total islet cross sectional area for each sample. Both measures were normalized to the total pancreas cross-sectional area.

Labeling of Intraislet Vasculature and Insulin Immunostaining

To detect intraislet vasculature, 100 μL of 1 mg/mL FITC-labeled tomato lectin (high affinity to rodent vascular endothelium; Vector Laboratories, Burlingame, CA) in PBS was injected intravenously into anesthetized mice and the pancreas immediately harvested into 10% buffered formalin for 24 h and processed for standard paraffin wax embedding. Sections (8 μm) were processed for antigen retrieval and immunostaining as previously described (10). Insulin was detected with guinea pig anti-insulin antibody (1:3,200; Abcam) followed by biotinylated donkey anti-guinea pig antibody (1:100; Abacus) and streptavidin-Cy3 (1:100; The Jackson Laboratory). Vascular-bound FITC-lectin was detected with rabbit anti-fluorescein (10 μg/mL; Life Technologies) followed by anti-rabbit Alexa 647 (10 μg/mL) and then DAPI (3 μmol/L; Sigma-Aldrich) to visualize cell nuclei. Images were taken with a confocal or multiphoton microscope (FV1000, Olympus; or LSM710NLO, Carl Zeiss).

In Vitro Matrigel Tube Formation Assay

MS1 cells were treated with 10 μmol S1P receptor inhibitor VPC23019 or vehicle (EtOH) for 30 min prior to seeding onto Growth Factor-Reduced Matrigel (1.5×10^4/well; Corning Life Sciences, Tewksbury, MA). The Matrigel tube formation assay was executed as previously described (27). Images were taken at 4 h using the EVOS XL Imaging System (Thermo Fisher Scientific, Waltham, MA). Images at ×10 magnification were used for publication. Tube formation was quantified by counting number of tubes per well using ImageJ (National Institutes of Health).

SK Activity Assay

Total SK activity was assayed using D-*erythro*-sphingosine (Cayman Chemical, Ann Arbor, MI) and [γ^{32}P]ATP (PerkinElmer, Melbourne, Victoria, Australia) as substrates, as described previously (17). SK activity was defined as

arbitrary radioactive spot intensity units per milligram protein of islet extract.

Statistics

WT and *Sphk1*-KO data sets were compared by unpaired *t* tests or one-way ANOVA. In the marginal mass transplantation model, percentage cure data were compared by the Gehan-Breslow-Wilcoxon test. Analyses were performed using Prism 5 for Windows (Version 5.04; GraphPad Software).

RESULTS

SK1 Is Expressed and Active in Isolated Islets

To characterize the expression of SK1 in pancreatic islets, mouse islets were isolated from C57B6 mice and cultured for 6–48 h prior to assessment of *Sphk1* gene expression by quantitative real-time PCR. Gene expression of *Sphk1* was detected, and, in fact, gene expression increased two- to threefold over a 48-h in vitro culture period (Fig. 1*A*). This time period is comparable to that experienced by human islets prior to clinical islet transplantation.

We next compared *Sphk1* gene expression in isolated islets and confirmed its ablation in the *Sphk1*-KO mice (Fig. 1*B*). Total SK enzymatic activity using thin-layer chromatography was then used to detect production of S1P in the lysates of whole pancreas or isolated islets and compared them between WT mice and those lacking SK1 (*Sphk1*-KO). As shown in Fig. 1*C*, total SK activity was reduced by 50% in whole pancreatic lysates from *Sphk1*-KO mice compared with WT mice, suggesting that half of the SK activity in the pancreas can be attributed to *Sphk1*, with the remainder from *Sphk2*. There was an even more marked reduction in SK activity in lysates from islets isolated from *Sphk1*-KO mice compared with WT (Fig. 1*D*), suggesting that SK1 activity is present in both exocrine and endocrine portions of the pancreas.

Sphk1-KO Mice Exhibit Normal Islet Function

Pancreata from WT and *Sphk1*-KO mice were examined histologically (Fig. 2*A* and *B*). Sections were stained for insulin expression to assess and compare islet number and size. There were no observable differences in the number of islets (Fig. 2*C*) or total insulin-producing islet area (Fig. 2*D*) between WT and *Sphk1*-KO pancreata. These data are consistent with our observations of normal glucose tolerance displayed by both WT and *Sphk1*-KO mice (Fig. 2*E* and *F*). We next subjected isolated islets to an in vitro glucose stimulation insulin secretion (GSIS) assay (Fig. 2*G* and *H*). Islets from WT and *Sphk1*-KO mice showed a

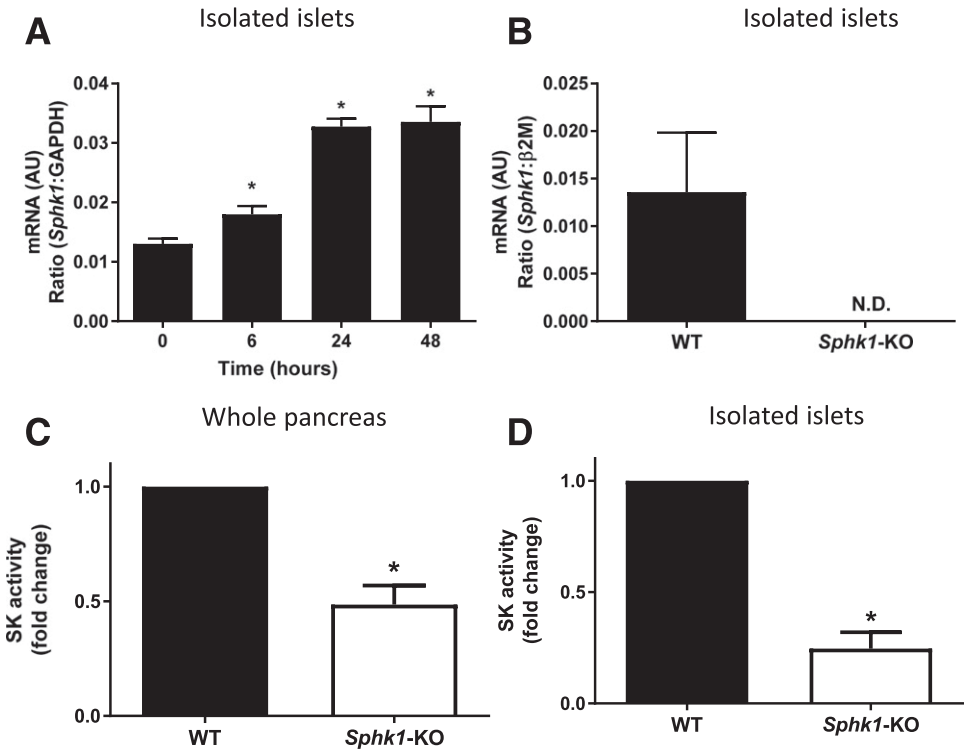

Figure 1—SK1 is expressed and active in pancreatic islets. In *A*, gene expression of *Sphk1* in cultured isolated islets from WT mice. RNA samples were collected at the indicated time points. Quantitative real-time PCR analysis was used to determine the fold change in *SphK1* relative to freshly isolated islets. Representative figure of three independent experiments, showing mean expression + SEM of triplicate samples. **P* < 0.05 vs. 0 h, one-way ANOVA with Dunnett multiple comparison test. In *B*, gene expression of *Sphk1* from isolated islets of WT and *Sphk1*-KO mice (n = 4 mice/group). In *C*, lysates from whole pancreas samples were isolated from WT (n = 6) or *Sphk1*-KO (n = 7) mice and assayed for SK activity, normalized to total protein from WT mice. Graph shows mean activity + SEM. **P* < 0.05 vs. WT, unpaired *t* test. In *D*, mean SK activity + SEM in islets isolated from WT and *Sphk1*-KO mice, expressed as the fold change in SK activity relative to WT islets; n = 3 islet preparations per group. **P* < 0.05 vs. WT, unpaired *t* test. AU, arbitrary units; N.D., not detected.

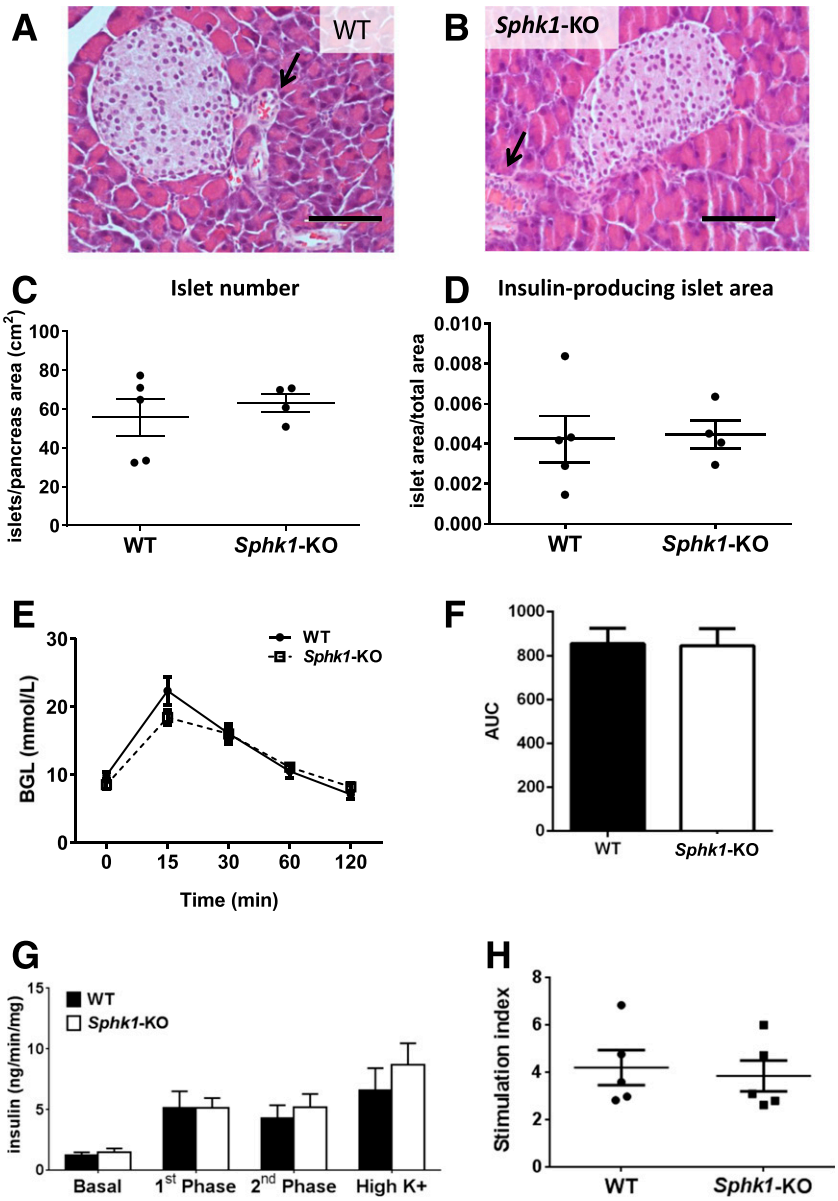

Figure 2—Characterization of pancreatic and islet function in *Sphk1*-KO mice. Conventional histological sections of pancreata from WT (*A*) or S*phk1*-KO (*B*) mice stained with hematoxylin and eosin. Islets were easily observable, often in close proximity to pancreatic blood vessels (arrow). Scale bars, 100 μm. Insulin immunolabeling in pancreata from WT (n = 5) or *Sphk1*-KO mice (n = 4) was examined at the fluorescence microscope to enumerate islet number (*C*) and islet area (*D*), normalized to total pancreas cross-sectional area. Calculations for individual mice shown, along with mean ± SEM. In *E*, glucose tolerance was measured in 16-week-old WT or *Sphk1*-KO mice following intraperitoneal injection of 2 mg/kg of glucose. BGL expressed as mean ± SEM; n = 5/group. In *F*, the AUCs from the glucose tolerance test were calculated for WT (black bar) and *Sphk1*-KO (white bar) mice. In *G*, glucose-stimulated insulin release was examined in islets isolated from WT (black bars) or *Sphk1*-KO (white bars) mice. Insulin released from groups of 10 islets in response to media (3 mmol/L glucose) for 1 h and high glucose (20 mmol/L) for 10 and 50 min was measured corresponding to basal, first-, and second-phase insulin release, respectively. n = 5/group; insulin secretion per minute was normalized to total protein content and expressed as mean + SEM. *H*: Stimulation indices were calculated (first-phase insulin secretion at 20 mmol/L glucose/basal insulin secretion at 3 mmol/L glucose) and mean ± SEM are shown. One-way ANOVA with Bonferroni multiple comparison test.

comparable ability to release insulin. These assays demonstrated normal gross anatomical appearance in islets from WT and *Sphk1*-KO mice, with appropriate response to glucose. Together, these data indicate a functional reduction in SK1 enzyme in *Sphk1*-KO islets, with maintained glucose responses in vitro and in vivo.

Intraislet Vascular ECs Are Reduced in *Sphk1*-KO Mice

With ever-increasing evidence that SK1 is important for vascular development and function (15,18,21,27,28), we next compared the vascularity of pancreatic islets from WT and *Sphk1*-KO mice. Murine pancreatic islets from both WT and *Sphk1*-KO mice contain functional

microvasculature as confirmed by the detection of intravenous injected FITC-lectin (Fig. 3*A*). To determine if the lack of SK1 affects intraislet vasculature, we compared the number of vascular ECs in isolated islets by flow cytometry. Examination of the first 10,000 events collected by flow cytometric analysis suggest that isolated islets from

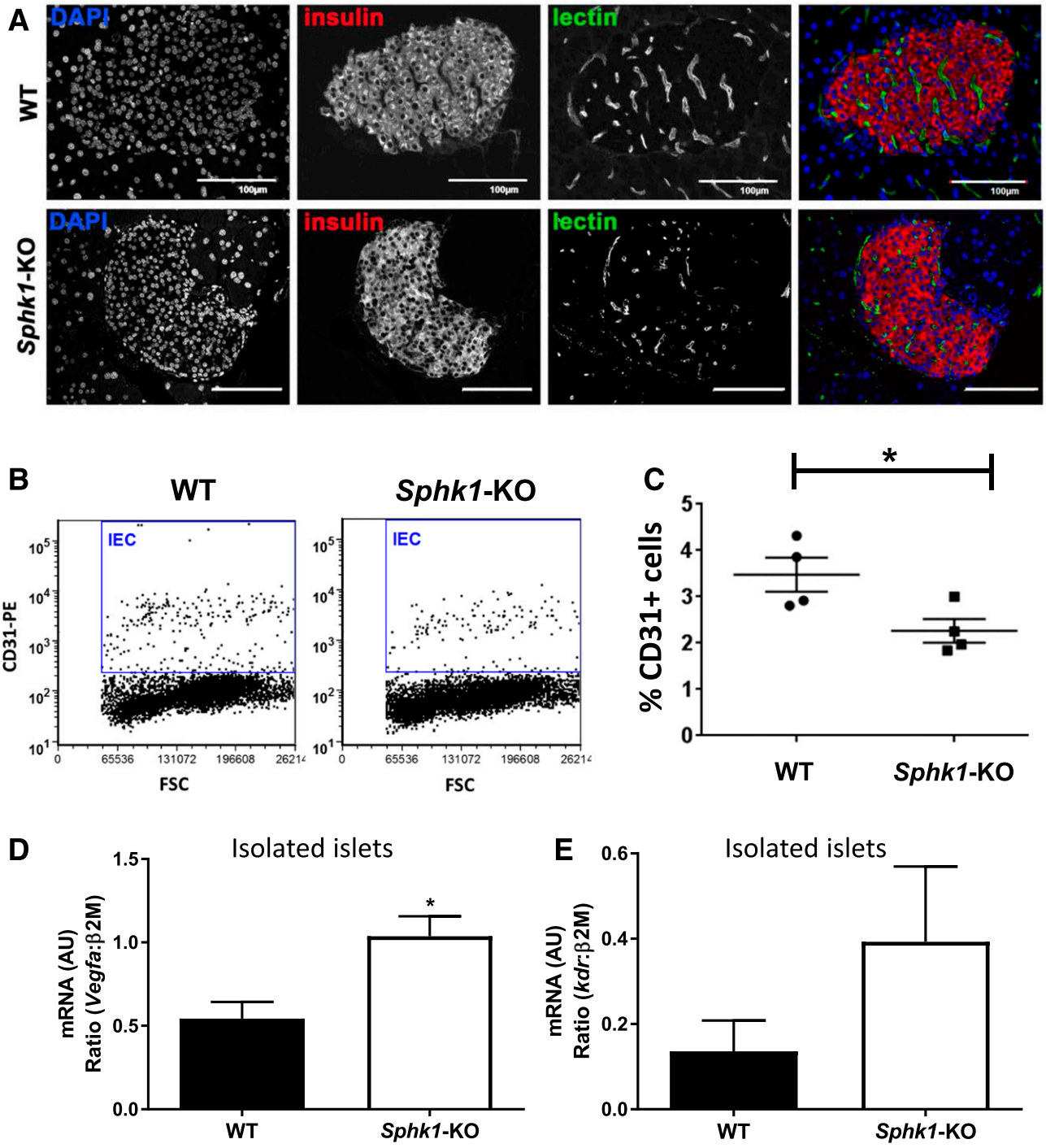

Figure 3—Intraislet vascular ECs in murine islets. Detection of patent microvessels within murine pancreatic islets by confocal microscopy. *A*: Cell nuclei (DAPI; blue), vasculature (intravital perfused FITC-lectin; green), and β-cells (insulin-Cy3; red) are shown in projected Z-stacks. Merged image containing all three channels is shown in color from WT and *Sphk1*-KO mice. In *B*, enumeration of intraislet ECs (IEC) in freshly isolated, dispersed islets as assessed by flow cytometry. Representative dot plots of 10,000 islet cells from WT and *Sphk1*-KO mice stained for CD31. IECs (CD31-positive) are indicated by the gating boxes. In *C*, comparison of mean ± SEM $CD31^+$ IEC numbers within the 10,000 analyzed by flow cytometry showed a significant decrease of IEC in *Sphk1*-KO islets ($n = 4$ animals/group; $^*P < 0.05$, unpaired, two-tailed *t* test). In *D*, gene expression of *Vegfa* from isolated islets of WT and *Sphk1*-KO mice ($n = 3$ to 4 mice/group; $^*P < 0.05$, unpaired, two-tailed *t* test). In *E*, gene expression of *kdr* from isolated islets of WT and *Sphk1*-KO mice ($n = 3$ to 4 mice/group; *P* not significant, unpaired, two-tailed *t* test). AU, arbitrary units; FSC, forward light scatter.

Sphk1-KO mice contain significantly fewer intraislet CD31-positive ECs when compared with an equal number of assessed islet-derived cells from WT mice (Fig. 3*B* and *C*). Interestingly, when islets are isolated from these mice, we observed a significant increase in gene expression of the proangiogenic growth factor *Vegfa* by the *Sphk1*-KO islets (Fig. 3*D*) as well as a trend for increased *kdr* (i.e., VEGF receptor 2) (Fig. 3*E*). This suggests that vascularity in isolated *Sphk1*-KO islets is reduced and potentially compromised by a hypoxic environment as indicated by an increase in *Vegfa* gene expression. Moreover, these results suggest that *Sphk1*-KO donor islets will contain fewer of the vascular building blocks that are known to contribute to revascularization posttransplantation (11,12).

Intraislet Vascular ECs Migrate via an S1P-Dependent Mechanism

To investigate whether the SK/S1P axis plays a role in the migration of intraislet vascular ECs, we used the xCELLigence RTCA DP Analyzer, which measures fluctuations in electrical impedance when a population of cells migrates across the electrodes repeatedly over time in culture. We found that the murine intraislet EC line MS1 migrated effectively over 12 h when S1P was present in the lower chamber compared with vehicle (Fig. 4*A*; single experiment representative of repeated experiments). When cells were incubated with the S1P receptor antagonist VPC23019 prior to their addition into the upper well, this migration was attenuated. When using the xCELLigence system, data are normalized to an initial time point to correct for seeding conditions. To examine the migration differences, we compared the slope of raw migration curves over the first 6 h, with Fig. 4*B* exemplifying a single experiment containing duplicate wells, which is representative of repeated experiments and illustrates the rate of migration independent of chosen normalization time point. These data support our observation that inhibition of S1P1 and/or S1P3 attenuate EC migration to S1P. Similarly, Fig. 4*C* shows that measurements of the AUCs of normalized data over 12 h (again, exemplified via duplicate readouts from a single experiment that is representative of repeated experiments) support a role for S1P/S1P receptors 1 and 3 in EC migration. Further analysis of MS1 to form vascular structures in vitro was achieved using a Matrigel angiogenesis assay, also in the presence or absence of the S1P receptor inhibitor VPC23019. When compared with vehicle treatment, MS1 cells exhibited a significantly reduced capacity to form tubules in the presence of VPC23019 (Fig. 4*D*, representative images from a single experiment, and Fig. 4*E*, pooled data from three biologically independent experiments). Importantly, we examined the effect of the S1P receptor inhibition on MS1 cell survival, and following 12-h exposure to VPC23019, flow cytometric analysis showed no alteration to cell survival as determined by staining for Annexin V and 7-AAD (Fig. 4*F*). Together, these data suggest that S1P is involved in the migration of intraislet ECs.

Sphk1-KO Islets Are Inferior for Reversing Diabetes in a Mouse Model

Because S1P receptor inhibitors reduce EC migration and tubule formation, we then sought to determine the importance of SK1 expression in islets posttransplantation and their efficiency to engraft. We compared islets from *Sphk1*-KO and WT mice in a syngeneic marginal mass islet transplant model (10), in which 200 islets were transplanted under the kidney capsule of streptozotocin-induced diabetic C57B6 mice. Transplantation with WT islets resulted in a 55% cure rate (five out of nine mice) by the end of the 28-day follow-up period (Fig. 5*A*). In contrast, transplanted islets from *Sphk1*-KO mice had a reduced capacity to cure diabetes, with one out of eight mice cured (13%) at 28 days posttransplantation (Fig. 5*B*). Statistical analysis of Kaplan-Meier curves showed a significant difference between WT and *Sphk1*-KO percentage cure rate (Fig. 5*C*). These in vivo data confirm that although a reduction in SK1 activity does not render pancreatic islets intrinsically dysfunctional, it does reduce their potency in controlling glycaemia in a diabetic syngeneic transplantation model.

DISCUSSION

Although there is compelling evidence that SK1 plays an important role in the pancreas and may be involved in the development of diabetes (29,30), there are limited data describing islet specific expression and activity. Components of the SK pathway, including SK1, SK2, and S1P receptors, have been detected within pancreatic islets in rats and mice (31,32). We showed that isolated murine pancreatic islets express SK1 at the mRNA and active protein level, and expression increases during early culture. This fits with previous reports demonstrating an increase in SK1 islet activity upon cytokine treatment (32), because cytokine release in islets is characteristic early postisolation (33). Whether this represents a protective response has been postulated, but remains unclear (34).

Islets from *Sphk1*-KO mice are less potent in restoring euglycemia in mice than WT islets. The SK pathway may affect islet transplantation in a number of ways. Firstly, physiological β-cell intracellular lipid signaling pathways may be directly influenced by SK activity, potentially altering glucose response and insulin release (35). Sphingolipid metabolism also overlaps with insulin production; genetic knockdown of *Sphk1* reduces insulin production in rat insulinoma lines (36), and exogenous S1P stimulates insulin secretion in isolated rodent islets (37). Also, high glucose increases SK activity and intracellular β-cell S1P levels in mouse islets and that knockdown of *Sphk2* impaired GSIS responses (38). However, we did not detect any intrinsic GSIS deficit in *Sphk1*-KO islets. Also, we found that *Sphk1*-KO mice had normal glucose tolerance. Differences in islet function in a transplant setting versus in situ may reflect

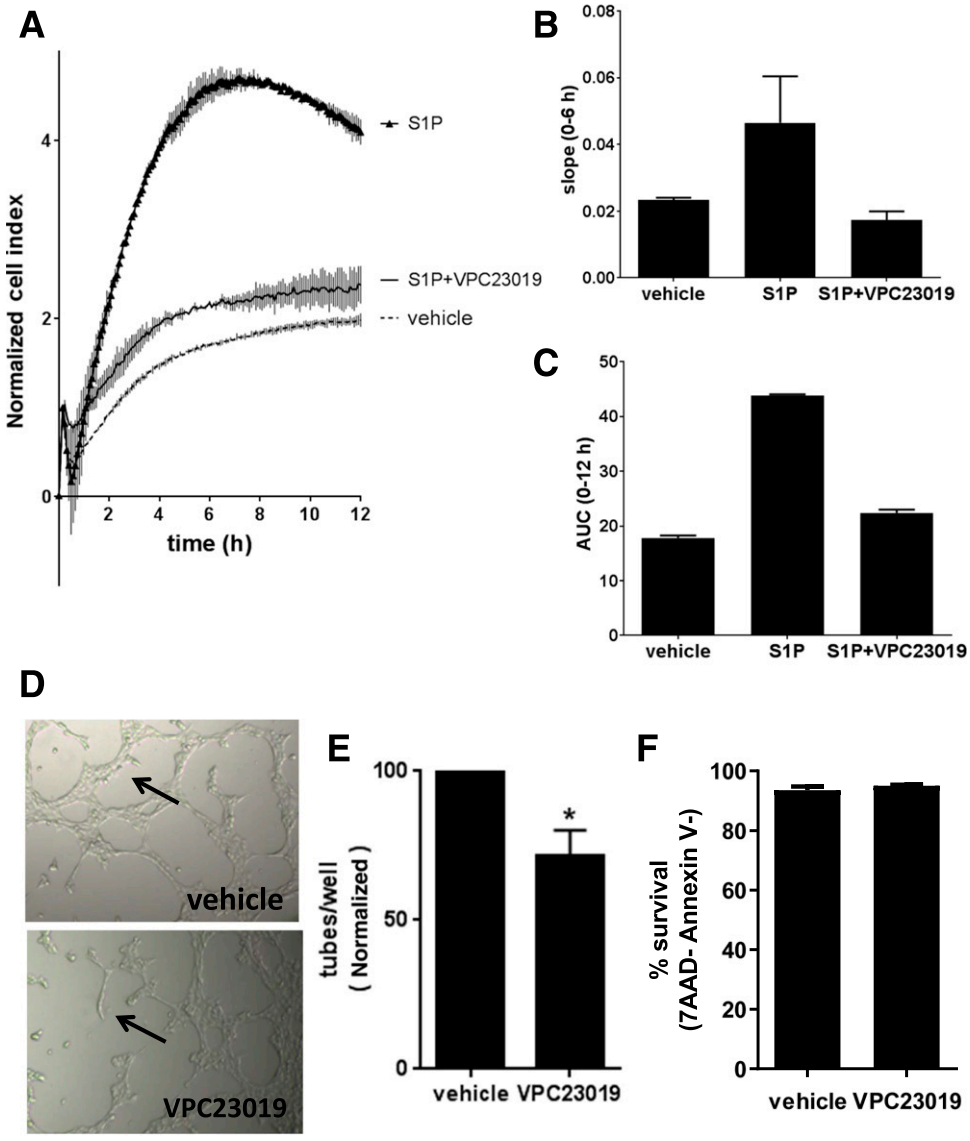

Figure 4—S1P receptor inhibitor reduces MS1 migration and tubule formation. *A–C*: Real-time monitoring of vascular EC (MS1) migration was examined in the xCELLigence System RTCA DP Instrument with a transwell setup (CIM-Plate16). *A*: Extent of migration over 12 h from the upper chamber in response to S1P (1 μmol/L) or vehicle in the lower chamber is detected as impedance changes and expressed as a mean cell index (± SD) normalized to initial well-seeding conditions. S1P receptor inhibitor (VPC23019 10 μmol/L) was preincubated with cells prior to assembly of chamber setup. $n = 2$ duplicate wells/condition; graph is representative of repeated experiments. Representative data from a single experiment with duplicate wells showing initial cell migration rate (slope of raw data over the first 6 h; *B*) and total cell migration (AUC of normalized data over the first 12 h; *C*) were calculated and are shown (mean + SD). *D* and *E*: The development of vascular tubes (arrows) by intraislet vascular ECs (MS1) was examined in vitro using Matrigel without or with the administration of S1P receptor inhibitor (VPC23019 10 μmol/L). $n = 3$ independent experiments. *$P < 0.05$ vs. vehicle. *F*: MS1 cells without and with VPC23019 (10 μmol/L for 12 h) were assessed for viability via staining for 7-AAD and Annexin V. $n = 3$ independent experiments.

differences in the islet mass in the particular model system. In *Sphk1*-KO animals, the collective β-cell mass of islets in situ may be able to overcome any impairment in individual islet function. In contrast, in our minimal mass model, reduced vascularity of the *Sphk1*-KO islet grafts may be insufficient to restore euglycemia.

SK pathway may affect islet transplantation via the action of local S1P, which is prosurvival in multiple cell types with direct addition of S1P in islet cultures protecting against cytokine-mediated apoptosis (31). Of the five S1P receptors, S1P receptors 1, 2, and 3 are expressed in rat β-cell lines or islets (39), suggesting that local S1P has the capacity to deliver signals at the β-cell surface. This is of particular interest, because in this study, we found that VPC23019, a selective antagonist of S1P receptors 1 and 3 (40), effectively blocked vascular responses of an islet EC line in vitro but was without effect on cell survival. Further genetic experiments will be required to define roles for S1P1 and/or S1P3 that are involved in these processes. Approaches to enhance revascularization have shown improvements in

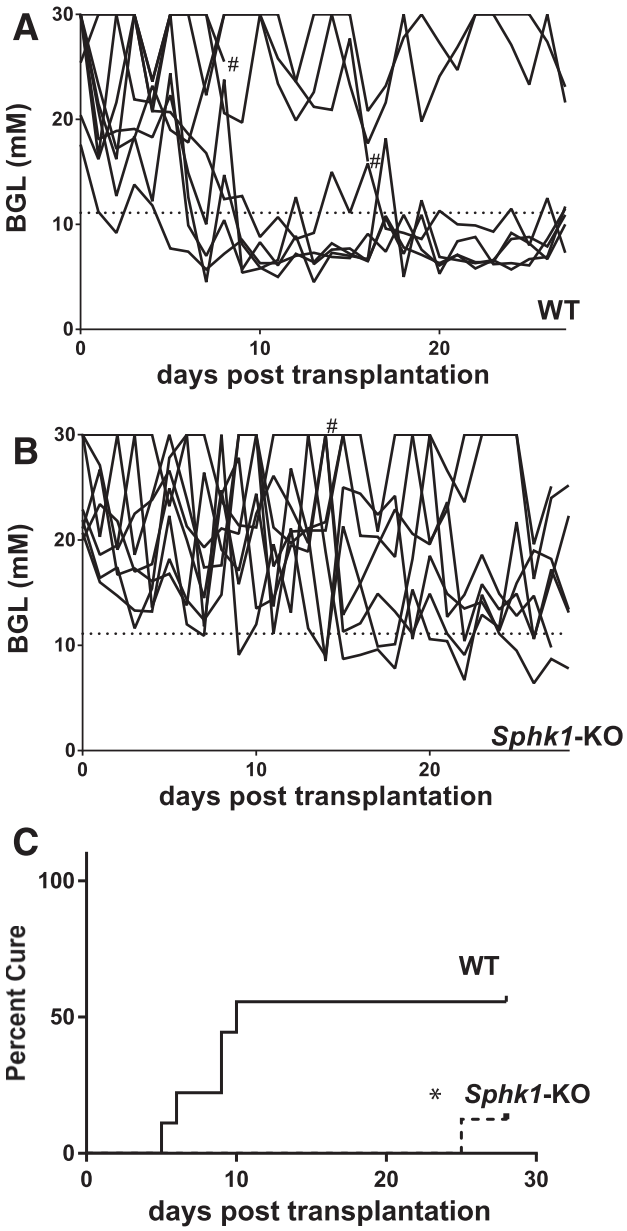

Figure 5—*Sphk1*-KO islets transplanted under the kidney capsule have a reduced capacity to cure diabetic mice. Diabetic C57B6 mice were transplanted with a minimal mass of islets (200) under the kidney capsule. BGLs in individual mice posttransplantation with WT islets (*A*; $n = 9$) or *Sphk1*-KO islets (*B*; $n = 8$) are shown. Cure was defined as two consecutive BGL readings <11.1 mmol/L (indicated by dashed line) with no subsequent sustained hyperglycemia. # denotes mouse was euthanized for poor health. In *C*, percentage cure of diabetic mice transplanted with minimal mass of islets displayed as Kaplan-Meier curves. *$P < 0.05$, Gehan-Breslow-Wilcoxon test.

diabetes cure rates in islet transplantation models. Overexpression of angiogenic factors improves transplant outcomes in mouse models (41,42), as have addition of extracellular matrix components or the cotransplantation of bone marrow–derived cells (10,43,44). SK and S1P promote angiogenesis (27,45), and in this study, we show intraislet ECs migrate toward S1P to form tubules in an S1P-dependent manner.

In this study, it was also observed that *Sphk1*-KO donor islets contained fewer resident ECs that are known to contribute to the revascularization of transplanted islets (11,12). Important to note is that the cytoarchitecture of pancreatic islets differ among species. For example, although human islets contain ~50% β-cells, and the α, β, and delta islet cells are intermingled throughout the islet and distributed along the blood vasculature in no discernable order (46,47), in the mouse, the islets contain ~80% β-cells, which are largely surrounded by the α and delta cells, and the islet vasculature is noticeably diminished in its content of contractile cells (i.e., smooth muscle cells and pericytes) (46–48). Irrespective of these differences, mouse islets remain the workhorse of islet biology research, and an important role for SK1 in islet transplantation has been revealed.

VEGF-A signaling is crucially important in pancreatic islets, and there is evidence in the literature of an overlap between the VEGF-A and SK pathways (49–54). Notably, we observed that islets isolated from *Sphk1*-KO mice exhibit an elevated mRNA level of *Vegfa*, as well as a trend for increased *kdr*, which supports an intrinsic mechanism to elevate the vascular content of the islets. Although the mechanisms and implications of elevating these genes remain to be determined, it is tempting to speculate that their increase is a direct consequence of a hypoxic environment in the *Sphk1*-KO mice, which results from the suboptimal pancreatic vasculature. This concept is supported by documented evidence of hypoxia-inducible factor response elements identified within the VEGF-A promoter region (reviewed in Metzger et al. [55]).

In our study, loss of SK1 in donor islets impaired their ability to cure diabetes in a syngeneic mouse model. This is likely because of diminished revascularization responses, reducing both the ingrowth of host vessels and the participation of resident donor-derived vasculogenic cells. Whether local S1P also directly affects β-cell apoptosis in the transplant setting is yet to be determined and an area under current investigation. With the advent of new pharmaceutical SK modulators and S1P receptor agonist/antagonists (56) or simply the ability to add exogenous S1P to islet isolation/transport media, the SK nexus represents a promising target for improving clinical islet transplantation.

Acknowledgments. The authors thank Pat Vilimas and Yvette DeGraaf from the Department of Anatomy & Histology, Flinders University, for technical assistance. The authors also thank Dr. Nikhil Thyagarajan, from the Centre for Cancer Biology, University of South Australia and SA Pathology, for technical assistance.

Funding. Channel 7 Children's Research Foundation, Diabetes Australia, and Royal Adelaide Hospital Research Fund grants supported this work. C.S.B. was supported by a Heart Foundation Fellowship (CR 10A 4983) and an Australian National Health and Medical Research Council project grant.

Duality of Interest. No potential conflicts of interest relevant to this article were reported.

Author Contributions. D.R.-C. designed and performed the experiments, analyzed data, and wrote the manuscript. D.P., K.K.M.M., and K.A.P. performed the experiments and analyzed data. H.P. performed the experiments, analyzed data, and reviewed and edited the manuscript. R.V.H. reviewed the manuscript. S.M.P. reviewed and edited the manuscript. C.D. designed the experiments and reviewed the manuscript. D.J.K. reviewed and edited the manuscript. S.T.G. reviewed the manuscript. P.T.C. conceived the experiments and reviewed and edited the manuscript. C.S.B. conceived and designed the experiments, analyzed data, and wrote and edited the manuscript. C.F.J. conceived, designed, and performed the experiments; analyzed data; and wrote the manuscript. C.S.B. and C.F.J. are the guarantors of this work and, as such, had full access to all of the data in the study and take responsibility for the integrity of the data and the accuracy of the data analysis.

Prior Presentation. Parts of this study were presented in abstract form at the 33rd Annual Scientific Meeting of The Transplantation Society of Australia and New Zealand, Canberra, Australia, 21–23 June 2016; the IPITA–IXA–CTS Joint Congress, Melbourne, Australia, 15–19 November 2015; and the 26th International Congress of The Transplantation Society, Hong Kong, 18–23 August 2016.

References

1. Hering BJ, Clarke WR, Bridges ND, et al.; Clinical Islet Transplantation Consortium. Phase 3 trial of transplantation of human islets in type 1 diabetes complicated by severe hypoglycemia. Diabetes Care 2016;39:1230–1240
2. Davalli AM, Scaglia L, Zangen DH, Hollister J, Bonner-Weir S, Weir GC. Vulnerability of islets in the immediate posttransplantation period. Dynamic changes in structure and function. Diabetes 1996;45:1161–1167
3. Emamaullee JA, Shapiro AM. Factors influencing the loss of beta-cell mass in islet transplantation. Cell Transplant 2007;16:1–8
4. Andersson A, Carlsson PO, Carlsson C, et al. Promoting islet cell function after transplantation. Cell Biochem Biophys 2004;40(Suppl.):55–64
5. Cantley J, Walters SN, Jung MH, et al. A preexistent hypoxic gene signature predicts impaired islet graft function and glucose homeostasis. Cell Transplant 2013;22:2147–2159
6. Peiris H, Bonder CS, Coates PT, Keating DJ, Jessup CF. The β-cell/EC axis: how do islet cells talk to each other? Diabetes 2014;63:3–11
7. Johansson A, Lau J, Sandberg M, Borg LA, Magnusson PU, Carlsson PO. Endothelial cell signalling supports pancreatic beta cell function in the rat. Diabetologia 2009;52:2385–2394
8. Nyman LR, Ford E, Powers AC, Piston DW. Glucose-dependent blood flow dynamics in murine pancreatic islets in vivo. Am J Physiol Endocrinol Metab 2010;298:E807–E814
9. Jansson L, Carlsson PO. Graft vascular function after transplantation of pancreatic islets. Diabetologia 2002;45:749–763
10. Penko D, Rojas-Canales D, Mohanasundaram D, et al. Endothelial progenitor cells enhance islet engraftment, influence β-cell function, and modulate islet connexin 36 expression. Cell Transplant 2015;24:37–48
11. Brissova M, Fowler M, Wiebe P, et al. Intraislet endothelial cells contribute to revascularization of transplanted pancreatic islets. Diabetes 2004;53:1318–1325
12. Nyqvist D, Köhler M, Wahlstedt H, Berggren PO. Donor islet endothelial cells participate in formation of functional vessels within pancreatic islet grafts. Diabetes 2005;54:2287–2293
13. Pitson SM. Regulation of sphingosine kinase and sphingolipid signaling. Trends Biochem Sci 2011;36:97–107
14. Allende ML, Sasaki T, Kawai H, et al. Mice deficient in sphingosine kinase 1 are rendered lymphopenic by FTY720. J Biol Chem 2004;279:52487–52492
15. Mizugishi K, Yamashita T, Olivera A, Miller GF, Spiegel S, Proia RL. Essential role for sphingosine kinases in neural and vascular development. Mol Cell Biol 2005;25:11113–11121
16. Sensken SC, Bode C, Nagarajan M, Peest U, Pabst O, Gräler MH. Redistribution of sphingosine 1-phosphate by sphingosine kinase 2 contributes to lymphopenia. J Immunol 2010;184:4133–4142
17. Sun WY, Dimasi DP, Pitman MR, et al. Topical application of fingolimod perturbs cutaneous inflammation. J Immunol 2016;196:3854–3864
18. Dimasi DP, Pitson SM, Bonder CS. Examining the role of sphingosine kinase-2 in the regulation of endothelial cell barrier integrity. Microcirculation 2016;23:248–265
19. Pitson SM, Moretti PA, Zebol JR, et al. Activation of sphingosine kinase 1 by ERK1/2-mediated phosphorylation. EMBO J 2003;22:5491–5500
20. Hsieh HL, Sun CC, Wu CB, et al. Sphingosine 1-phosphate induces EGFR expression via Akt/NF-kappaB and ERK/AP-1 pathways in rat vascular smooth muscle cells. J Cell Biochem 2008;103:1732–1746
21. Bonder CS, Sun WY, Matthews T, et al. Sphingosine kinase regulates the rate of endothelial progenitor cell differentiation. Blood 2009;113:2108–2117
22. Lin CI, Chen CN, Lin PW, Lee H. Sphingosine 1-phosphate regulates inflammation-related genes in human endothelial cells through S1P1 and S1P3. Biochem Biophys Res Commun 2007;355:895–901
23. Jessup CF, Bonder CS, Pitson SM, Coates PT. The sphingolipid rheostat: a potential target for improving pancreatic islet survival and function. Endocr Metab Immune Disord Drug Targets 2011;11:262–272
24. Pfaffl MW. A new mathematical model for relative quantification in real-time RT-PCR. Nucleic Acids Res 2001;29:e45
25. Livak KJ, Schmittgen TD. Analysis of relative gene expression data using real-time quantitative PCR and the 2(-Delta Delta C(T)) method. Methods 2001;25:402–408
26. Arbiser JL, Moses MA, Fernandez CA, et al. Oncogenic H-ras stimulates tumor angiogenesis by two distinct pathways. Proc Natl Acad Sci U S A 1997;94:861–866
27. Parham KA, Zebol JR, Tooley KL, et al. Sphingosine 1-phosphate is a ligand for peroxisome proliferator-activated receptor-γ that regulates neoangiogenesis. FASEB J 2015;29:3638–3653
28. Sun WY, Pitson SM, Bonder CS. Tumor necrosis factor-induced neutrophil adhesion occurs via sphingosine kinase-1-dependent activation of endothelial alpha5beta1 integrin. Am J Pathol 2010;177:436–446
29. Bruce CR, Risis S, Babb JR, et al. Overexpression of sphingosine kinase 1 prevents ceramide accumulation and ameliorates muscle insulin resistance in high-fat diet-fed mice. Diabetes 2012;61:3148–3155
30. Qi Y, Chen J, Lay A, Don A, Vadas M, Xia P. Loss of sphingosine kinase 1 predisposes to the onset of diabetes via promoting pancreatic β-cell death in diet-induced obese mice. FASEB J 2013;27:4294–4304
31. Laychock SG, Sessanna SM, Lin MH, Mastrandrea LD. Sphingosine 1-phosphate affects cytokine-induced apoptosis in rat pancreatic islet beta-cells. Endocrinology 2006;147:4705–4712
32. Mastrandrea LD, Sessanna SM, Laychock SG. Sphingosine kinase activity and sphingosine-1 phosphate production in rat pancreatic islets and INS-1 cells: response to cytokines. Diabetes 2005;54:1429–1436
33. Cowley MJ, Weinberg A, Zammit NW, et al. Human islets express a marked proinflammatory molecular signature prior to transplantation. Cell Transplant 2012;21:2063–2078
34. Boslem E, Meikle PJ, Biden TJ. Roles of ceramide and sphingolipids in pancreatic β-cell function and dysfunction. Islets 2012;4:177–187
35. Sjöholm A. Intracellular signal transduction pathways that control pancreatic beta-cell proliferation. FEBS Lett 1992;311:85–90
36. Hasan NM, Longacre MJ, Stoker SW, et al. Sphingosine kinase 1 knockdown reduces insulin synthesis and secretion in a rat insulinoma cell line. Arch Biochem Biophys 2012;518:23–30
37. Shimizu H, Okajima F, Kimura T, et al. Sphingosine 1-phosphate stimulates insulin secretion in HIT-T 15 cells and mouse islets. Endocr J 2000;47:261–269
38. Cantrell Stanford J, Morris AJ, Sunkara M, Popa GJ, Larson KL, Özcan S. Sphingosine 1-phosphate (S1P) regulates glucose-stimulated insulin secretion in pancreatic beta cells. J Biol Chem 2012;287:13457–13464
39. Laychock SG, Tian Y, Sessanna SM. Endothelial differentiation gene receptors in pancreatic islets and INS-1 cells. Diabetes 2003;52:1986–1993

40. Davis MD, Clemens JJ, Macdonald TL, Lynch KR. Sphingosine 1-phosphate analogs as receptor antagonists. J Biol Chem 2005;280:9833–9841
41. Lai Y, Schneider D, Kidszun A, et al. Vascular endothelial growth factor increases functional beta-cell mass by improvement of angiogenesis of isolated human and murine pancreatic islets. Transplantation 2005;79:1530–1536
42. Olsson R, Maxhuni A, Carlsson PO. Revascularization of transplanted pancreatic islets following culture with stimulators of angiogenesis. Transplantation 2006;82:340–347
43. Kang S, Park HS, Jo A, et al. Endothelial progenitor cell cotransplantation enhances islet engraftment by rapid revascularization. Diabetes 2012;61:866–876
44. Oh BJ, Oh SH, Jin SM, et al. Co-transplantation of bone marrow-derived endothelial progenitor cells improves revascularization and organization in islet grafts. Am J Transplant 2013;13:1429–1440
45. Ancellin N, Colmont C, Su J, et al. Extracellular export of sphingosine kinase-1 enzyme. Sphingosine 1-phosphate generation and the induction of angiogenic vascular maturation. J Biol Chem 2002;277:6667–6675
46. Brissova M, Fowler MJ, Nicholson WE, et al. Assessment of human pancreatic islet architecture and composition by laser scanning confocal microscopy. J Histochem Cytochem 2005;53:1087–1097
47. Cabrera O, Berman DM, Kenyon NS, Ricordi C, Berggren PO, Caicedo A. The unique cytoarchitecture of human pancreatic islets has implications for islet cell function. Proc Natl Acad Sci U S A 2006;103:2334–2339
48. Nyman LR, Wells KS, Head WS, et al. Real-time, multidimensional in vivo imaging used to investigate blood flow in mouse pancreatic islets. J Clin Invest 2008;118:3790–3797
49. Brissova M, Shostak A, Shiota M, et al. Pancreatic islet production of vascular endothelial growth factor–a is essential for islet vascularization, revascularization, and function. Diabetes 2006;55:2974–2985
50. Igarashi J, Erwin PA, Dantas AP, Chen H, Michel T. VEGF induces S1P1 receptors in endothelial cells: Implications for cross-talk between sphingolipid and growth factor receptors. Proc Natl Acad Sci U S A 2003;100:10664–10669
51. Kamba T, Tam BY, Hashizume H, et al. VEGF-dependent plasticity of fenestrated capillaries in the normal adult microvasculature. Am J Physiol Heart Circ Physiol 2006;290:H560–H576
52. Lee H, Lee JK, Park MH, et al. Pathological roles of the VEGF/SphK pathway in Niemann-Pick type C neurons. Nat Commun 2014;5:5514
53. Reinert RB, Brissova M, Shostak A, et al. Vascular endothelial growth factor-a and islet vascularization are necessary in developing, but not adult, pancreatic islets. Diabetes 2013;62:4154–4164
54. Zhang N, Richter A, Suriawinata J, et al. Elevated vascular endothelial growth factor production in islets improves islet graft vascularization. Diabetes 2004;53:963–970
55. Metzger CS, Koutsimpelas D, Brieger J. Transcriptional regulation of the VEGF gene in dependence of individual genomic variations. Cytokine 2015;76:519–526
56. Khattar M, Deng R, Kahan BD, et al. Novel sphingosine-1-phosphate receptor modulator KRP203 combined with locally delivered regulatory T cells induces permanent acceptance of pancreatic islet allografts. Transplantation 2013;95:919–927